Chapter 23
II–VI Semiconductor QDs in Surface Plasmon Resonance Sensors

Hina F. Badgujar and Anuj K. Sharma

23.1 Introduction: Principles of Surface Plasmon Resonance (SPR)

Surface plasmon resonance (SPR) sensor platform works on optical theory to measure the refractive index (RI) variation within the range of the surface plasmon field, which extends up to ~300 nm away from the sensor surface (x- and y-axis direction) and is equivalent to an evanescent wave (EW). The penetration depth of EW depends on the wavelength of incident light and it decays exponentially in the direction of the z-axis with the distance from the interface. In order to generate a plasmonic field at the metal-dielectric interface, the momentum of the incoming light must match with the momentum of the conduction band electrons. When the coupling condition is satisfied at a particular angle and wavelength, the light is converted very effectively into surface plasmon waves (SPW). This phase matching is achieved through the phenomenon of attenuated total reflection (ATR) at smooth flat surfaces. It generally requires a higher RI material (Fig. 23.1a). The matching condition may be interpreted according to the dispersion relation given by Raether et al. [59]:

$$K_{spp} = \frac{2\pi}{\lambda_0}\sqrt{\frac{\varepsilon_m \varepsilon_d}{\varepsilon_m + \varepsilon_d}} = \frac{2\pi}{\lambda_0} n_p \sin\theta_i \tag{23.1}$$

H. F. Badgujar
Central University of Gujarat, Gandhinagar, India

A. K. Sharma (✉)
National Institute of Technology Delhi, Delhi, India
e-mail: anujsharma@nitdelhi.ac.in

G. Korotcenkov (ed.), *Handbook of II-VI Semiconductor-Based Sensors and Radiation Detectors*, https://doi.org/10.1007/978-3-031-24000-3_23

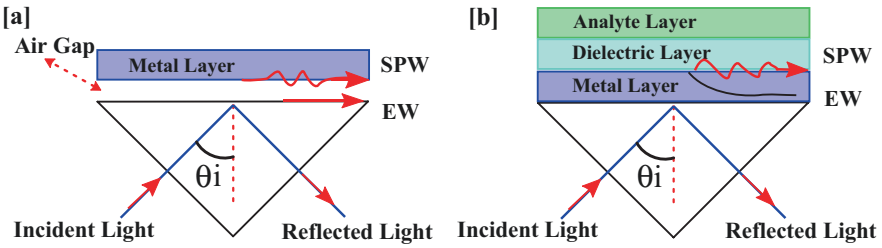

Fig. 23.1 Otto (**a**) and Kretschmann (**b**) configuration. EW stands for Evanescent Wave and SPW refers to the surface plasmon wave

where n_p is the RI of the coupling prism, θ_i is the incident angle of light, ε_m is the dielectric constant of metal, ε_d is the dielectric constant of dielectric and K_{spp} is the wave vector of surface plasmon. The biosensing mechanism takes place by detecting the analytes layer adjutant to the metal-dielectric layer with the EW through the interaction of light (Fig. 23.1b). In the plasmon resonance condition, any minute changes in RI can be monitored in terms of variations in intensity, wavelength, or angular shift for sensing purposes. Here ε_m depends on the wavelength of the incident light, and ε_d depends on the RI of the dielectric environment.

Further, in order to generate localised surface plasmon resonance (LSPR), particularly around the nanoparticle vertices, the external electric field can be applied to "nano-islands" of NPs. These islands induce very strong surface plasmon field gradients that could potentially lead to a phenomenon of light entrapment. When this occurs, the electron clouds of nano-islands encounter combined harmonic oscillations and are smaller than the light wavelength, typically in the Mie scattering region. NPs of gold (Au) and silver (Ag) are generally used to produce the strongly localised electromagnetic field with very high intensity.

SPR biosensing platform can be designed using different transducer configurations, such as the conventional Kretschmann configuration, including ATR, fibre-optic configuration, lossy mode resonances (LMRs) and SPR imaging (SPRi). Recently, it has been observed that the optical sensor design based on LSPR, long-range SPR (LRSPR), optical waveguide, optical resonator and photonic crystal (PC) are capable of providing enhanced sensing performance in comparison to the conventional SPR configuration (Fig. 23.2).

For SPRi, the phase or reflectivity is measured by a collimated beam of light passing through a prism and is rendered incident on a deposited plasmonic film. The reflected light is then detected with a CCD camera after crossing a narrow band interference filter, and an SPR image of the surface is thus obtained [30]. Among others, semiconducting NPs embedded transducer systems are of great importance in medical diagnostics and therapeutics. These solid-state SPR sensors provide new insights and information for understanding the effects of monitoring molecular interactions by RI increment on signal changes. These NPs are assumed to have the freedom to oscillate under the influence of the EW created by surface electrons. Collective oscillations of such surface electrons are highly sensitive to the RI

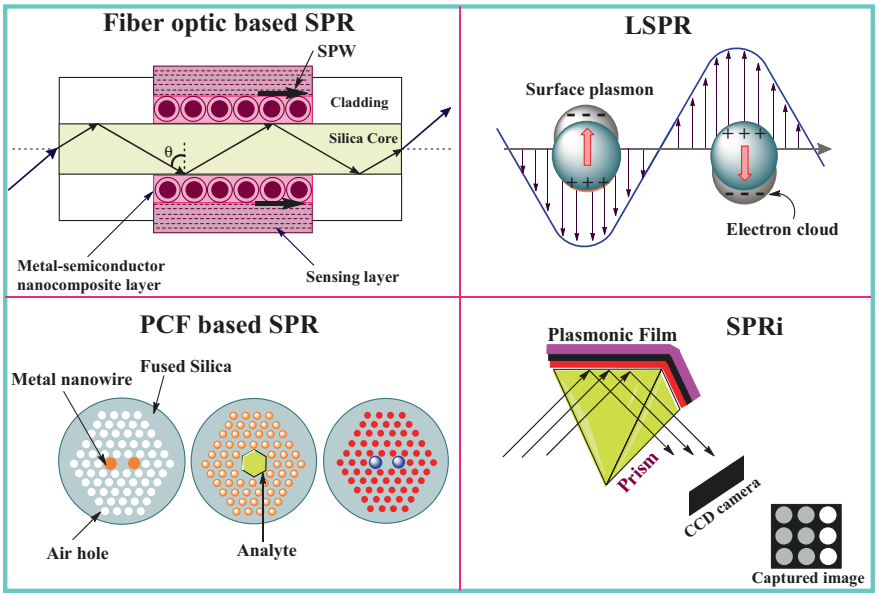

Fig. 23.2 Design of SPR biosensor-based quantitative platforms for biomolecular detection

changes, which can be directly correlated with the mass density changes on a sensor surface, and can be used to measure real-time biomolecular interactions and quantification events [24, 53]. Classical models offer a qualitative approximation for understanding the biomolecule interaction. In this way, several approximations and models have been applied to transform a biomolecular binding event or biological reaction into a physically measurable signal [43].

Semiconductor plasmonicbiointerfaces are often designed with regenerative surface chemistry, allowing multiple interactions without loss of reactivity. The biointerface design typically consists of three essential components integrated into a single system: the optical setup, the fluid handling chamber and the sensing surface. The sensor configuration offers a physical barrier between the optical setup (dry portion) and the measurement chamber (wet portion). The characteristic of the biosensor has a major impact on the measurement of biological interaction. The importance of light interaction in a biophysical interface is an important area of research in the scientific community. However, the toughest task is to indulge the clinicians and clinical chemists in the functioning principles and assure them about its benefits. The non-invasive and label-free technology may be advantageous to exploit its acceptance by the healthcare industry in the near future biopsy technique. The following are the main components to fabricate the biosensor for biomedical applications and clinical prospects:

- Plane polarised incident wave that should be operated in the red and infrared region
- The thin film formation of plasmonic material (Au/Ag nanoarray)
- Coupling prism with a higher RI

Some components may vary according to the requirement of the applications. Many researchers have investigated nanostructure semiconductors for various biotechnological and optical sensing applications, and in this regard, the quantum dots (QDs) induce a dominant tunable LSPR. Over the last decades, the exploitation of QDs in a biosensor has been very prominent for probing biological processes and the associated biological surroundings effect in real-time measurement. Owing to its careful monitoring of biomolecules and high selectivity with a label-free approach, it has been extensively used to analyse the kinetics of biomolecular interactions such as lipid membrane-protein interactions [3], virus detection [71], hybridisation of DNA [24] and protein/polymer adsorption [11].

While fabricating SPR sensors, there are a few crucial parameters such as sensitivity, signal-to-noise ratio, accuracy, precision and response time that need to be taken into account and, to be calibrated with standard methods. The plasmon depth must be short enough to allow the molecular binding event to fill most of the plasmon field. However, it is not too short for the binding event to occur outside the plasmonic field. Therefore, the penetration depth must be optimal in the range of 10 to 20 nm. These parameters are strongly dependent on the measurement method, the preferred optical platform and selection of the deposited layer (as NPs, thin-films and pores nanomaterials) and even on the operational parameters (excitation wavelength, detector efficacy, etc.). Moreover, sensing ability such as cross-sensitivity or selectivity relies on the affinity between the bio-marker and the bio-receptor, as well as the environmental conditions (e.g. in vivo or in vitro) in which the sensor is being

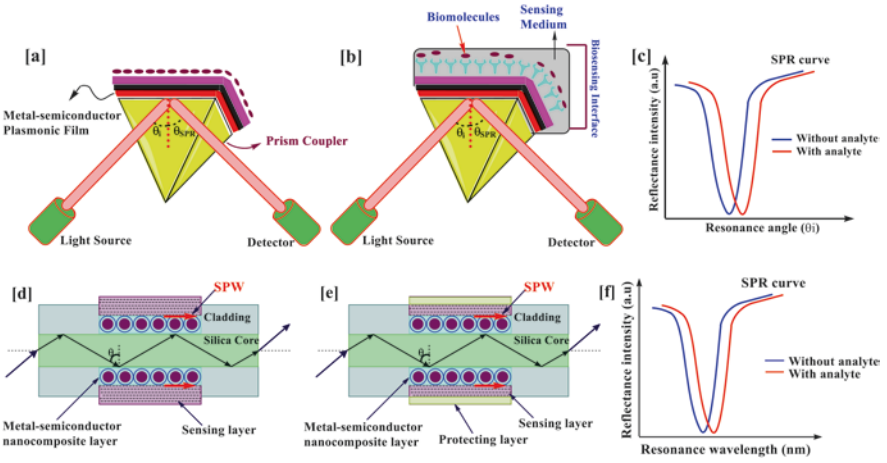

Fig. 23.3 Schematic representation of the Kretschmann configuration-based SPR biosensor. Prism-based SPR sensor consists of a prism (**a**), biomolecules and analyte layers (**b**) and its SPR curve when RI changes in the presence of analyte (**c**); and fibre optic SPR sensor with core–shell metal-semiconductor nanocomposite layer (**d**) sensing region coated with protecting layer (**e**) and its SPR curve when RI changes in the presence of analyte (**f**). Here, SPW stands for surface plasmon wave, which exists at the interface of the metal-semiconductor nanocomposite layer and the adjacent sensing layer

operated. For instance, experiments can be done under controlled buffer (PBS) conditions (Fig. 23.3), or in more complex matrices such as blood serum, plasma or blood itself [21]. Metal films corrode into biological solutions, thus, reducing the quality factor and the darkness of plasmon resonances and sensitivity. The use of semiconductor layer on the metallic film extends the range of metals that can be used for plasmonbiosensing and increases sensitivity by higher orders of magnitude [96]. It promises the stability of metal in a liquid and preserves plasmonic resonance under biofunctionalisation [90]. Essential parameters, for example, regeneration, repeatability, or reproducibility, are highly dependent on the testing chip and, consequently, introducing external bio-agents, like enzymes, that can disturb the already functionalised bioreceptors or biomarker connection to start the detection process again.

As the complexity of the experimental medium increases, it is necessary to handle the potential number of difficulties, since many other biomolecules can trigger the reaction by interfering with the detection of analyte solution [6].

The planar geometry of SPR lends itself well to multilayer structures to enrich the biological sensitivity. Accordingly, multilayer approaches have generally been demonstrated in prism-coupled systems and adapted for boosting the SPR biosensor performance [58]. However, the difficulty lies in incorporating the biofunctionalised sensing layer without disturbing the optical properties of the multilayer. The semiconductor NPs layers between the metal coating and the bio-receptors determine the biomolecules immobilisation and provide new avenues for achieving biodetection selectivity [67]. The performance is commonly measured in terms of RI sensitivity, RI resolution and figure of merit (FOM). An optimal biosensor would have enormous RI sensitivity (leading to an extremely fine RI resolution) with a narrow plasmon resonance for high FOM defined as:

$$\text{FOM} = \frac{\text{Sensitivity}}{\text{FWHM}} \tag{23.2}$$

In the above expression, FWHM is the full width of the plasmon band at half maximum. The improvement in sensor design is the most exciting research field in biomedical application and clinical chemistry, especially for LSPR sensors. Regardless of these, the plasmon resonance should ideally be tuned into the biological window in the near-infrared (NIR) region to avoid spectral interference to detect LSPR resonance in biofluids. Many strategies to enhance biological interaction have been demonstrated. Here, a fibre optic SPR probe with metal (core) semiconductor (shell) nanocomposite design based on wavelength and angular mode is shown (see Fig. 23.3d, e) [65]. The effect ofNP diameter, thickness of the sensing layer and their surrounding curvature on sensor's performance were studied in this work [65]. Four types of spherical shape semiconductor materials, namely, cadmium sulphide (CdS), cadmium selenide (CdSe), lead sulphide (PbS) and zinc oxide (ZnO) are taken into account for the plasmonic resonance. In further work, different values of RI for different sensing layers are also considered for the core–shell NPs. However, a more practical difficulty is their stability while performing an

in vivo test. As a result, the signal does not suffer from light scattering through the very dense matrix. To achieve this objective, measurements in undiluted biological fluids, long-term stability in complex matrices and integration into the body are vital.

To access the biological window, semiconducting NPs are currently considered to achieve higher sensitivity and resonances in the infrared region [5, 41]. It is important to note that in vivo biosensors may be used to continuously monitor therapeutic concentrations of drugs with a narrow therapeutic range. Therefore, more advanced spectroscopic techniques needed to be applied for accurate determination of particles size, concentration and deformations at biointerfaces [60]. Conceivably, semiconductor nanostructures could provide unperturbed light intensities at different measurement angles or wavelengths, thereby reducing signal drift arising from biointerferences at the sensor design level.

23.2 SPR-Based Biosensors

The basic functionality of an SPR biosensor is to analyse the kinetics of biomolecular events in the presence of biochemical target analytes for performing the wide ranges of clinical tasks such as imaging, detection, recognition and monitoring of different tissues and organs. SPR sensors facilitate noninvasive, label-free and rapid biological response during the biomolecular binding events in real-time analysis. For label-free real-time detection, the physicochemical transduction method is utilised to convert the biological signal into an accurate electronic signal based on the biosignalling of the analytes. These signals carry helpful information (i.e. quantitative analysis of targeted analyte or group of analytes) in understanding the physiological mechanisms of a specific event or biological system. The application of SPR biosensing can be helpful in real-time medical diagnosis using portable point-of-care devices.

In order to acquire basic knowledge about the SPR operation, a fundamental understanding of the optics is sufficient, as we have discussed in an earlier section. The result for the sensor chip based on the metal interface is broadly achievable in all aspects, but the metal-semiconductor nanoplasmonic interface offers good performance owing to recent chip progression [1, 45, 66, 94]. The semiconductor medium leads to a rapid injection of the charge carriers into the metal to produce an enormous plasmonic response and quantum efficiency [65]. The coupling of the SPW and the electromagnetic behaviour of the background medium could be expected to produce a tunable optical response with a dominant LSPR. Thus, the collective and coherent oscillation of electrons across the NPs upon the interaction with light at a specific resonant wavelength causes LSPR phenomena (Fig. 23.4). The plasmonic resonance can be influenced by the diameter and doping concentration and the nature of the composition, including the inter-particle distance [80]. To manifest a resonance effect, an appropriate selection of NP is significant for achieving excellent sensing performance.

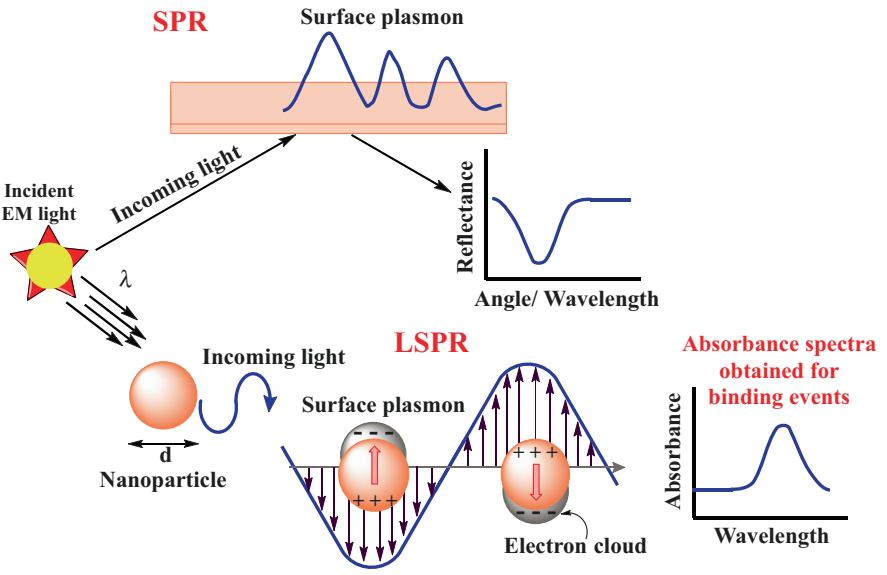

Fig. 23.4 Schematic of surface plasmon oscillations in prism coupling configuration and localised surface plasmon on NP. Incoming light impinges on a thin metallic film deposited on a prism surface where the p-polarised light absorbed by the surface plasmon is seen from a minimum in the reflection spectra. In LSPR, a confined oscillation of the surface plasmon in the NP surface is generated corresponding absorbance spectra for binding events on NPs

NP-based optical platforms have received considerable interest due to their higher sensitivity and selectivity. Interesting developments have been carried out concerning the application in metallic semiconductor NP-based biosensors. The use of various metal-semiconductor nanostructures has resulted in faster detection, low-cost manufacturing, reproducibility, flexibility and adequate sensitivity. In this context, near-field enhancement and high LSPR characteristics of metal-semiconductor NPs were studied theoretically and experimentally for plasmon-related applications [1, 17, 19, 65, 72]. The enhanced plasmonic behaviour of NPs depends on geometric morphology (i.e. sphere, cubic, tubular, tetrahedron and octahedron), matrix structure (i.e. rigid sphere, hollow core and core–shell) and composition of NPs, excitation wavelength, as well as the local dielectric environment [63, 89, 95].

The concept of light interaction and plasmonic oscillations in metal-semiconductor-based nanosystem has received much attention in the fabrication of SPR biosensors [57]. Also, the coupling of plasmonic and semiconducting features could lead to tunable photoluminescence (PL), large resonance Raman scattering and ultimate linear/non-linear optical characteristics. Plasmonic properties of semiconductors are suitable for NIR and mid-infrared (MIR) wavelength sensing applications [9]. Quantum effects gain importance for NPs, when electron tunnelling across the dielectric barrier occurs in the minimal gap. Electronic tunnelling reduces the magnitude of total mode splitting with an additional narrowing of the gap and field improvement compared to conventional predictions. Metal NPs can be

incorporated into a semiconductor matrix using experimental methods, resulting in higher extinction, more scattering quantum efficiency and more remarkable field improvement than metallic NPs [98]. In particular, LSPR peak shifts caused by RI changes have been found useful in detecting various biochemical changes occurring at the cellular scale [16, 81]. Here, the important and excellent photonics characteristics of nanocrystalline semiconductor materials have been explained in detail. These electron-hole carrier nanomaterials provide the perspective of additional exotic properties such as CdSe, CdTe, CdS, ZnS and QDs, and in enhancing the local electromagnetic field with longer plasmon wavelength, superior polarities and high curvatures.

The leading sensory components are biological machines like whole cells, tissues, enzymes, antibodies, antigens, receptors, nucleic acids, microorganisms and organelles (Fig. 23.5). They generate biosignals in the specific interaction between the target analytes and biological system. Thus, the biological signal has passed through the physiological system's proximity and is immensely important for medical diagnosis. Potential bimolecular interactions include affinity, kinetics, thermodynamics and analysis of the specificity and concentration of interacting molecules. In general, biological and biochemical interactions occur when the analyte RI ranges from 1.33 to 1.36 [28]. Higher detection accuracy and sensitive

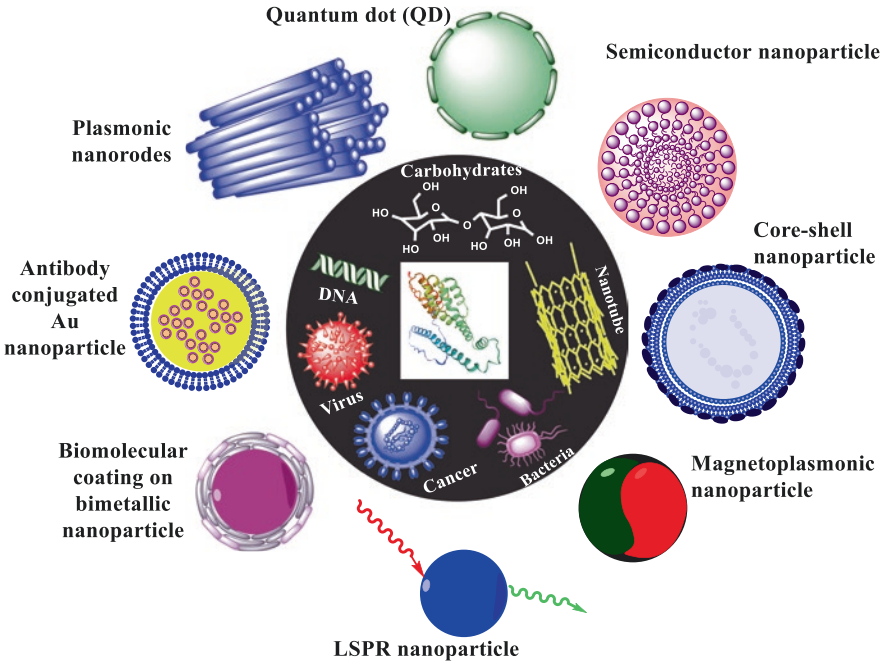

Fig. 23.5 Nanoscale materials that have been explored to design SPR biosensors, and their performance play leading role in profiling biomolecules binding or cellular events, such as, carbohydrates, protein, DNA/miRNA, bacteria viruses and tumour cells

functioning of sensors emerged as ideal devices for clinical monitoring biomolecules in a series of medical conditions (i.e. Alzheimer's disease, tumour, diabetes, hepatitis, leukaemia, etc.). A different class of bio-analytes has been extensively studied on SPR-based biosensor platforms [14, 22, 31].

Accordingly, it has been explored to detect tumour biomarkers [55], including proteins/enzymatic interaction [27], antigen-antibody binding [81], therapeutic drug sensing [87], monitoring metabolite pathway [13], hormones, miRNA, DNA [70] and among other active biomarkers detection [2, 36, 47]. Still, the active researches on the detection of such biomarkers are very broad, and the contemporary sensor design yet needs to be improved. As per one such work, nearly 64% of the money involved in the market is due to activities related to medicine: home healthcare and point-of-care testing [68]. Core–shell nanostructure paves significant interest due to the geometric parameters (core diameter and shell thickness) and hence, used in many modern medical diagnostic devices in recent years. The effects of the thickness of the internal core, the outer diameter of the shell layer, and the superior quantum efficiency have essentially shown tunable plasmonic bands based on Mie's theory. Thus, varying geometrical parameters of core–shell structure can render the shift with an increment in scattering intensity [13]. Higher-order plasmonic excitation can be achieved by forming large NPs, and by exploiting short and long-range interactions, the latter spectra become more complicated than pure/single NPs [25, 83]. In most cases, SPR of core–shell NPs is red-shifted over a broad spectrum range from the visible to infrared by merely increasing core diameter or shell thickness.

23.3 SPR in II–VI Semiconductor QDs

Conventional plasmonic NPs are used for biosensing applications and perform well in the visible and near-infrared region but they demonstrate limitations especially at higher wavelengths due to intrinsic losses [93]. The research of tunable and suitable materials is an essential requirement for creating biosensors for the IR environment. A number of the proposal have been made for alternative plasmonic materials, such as Group IV materials and II–VI semiconductors, where, in particular, InAs have excellent properties [5, 39, 41]. NPs with a CdS and CdSe core in particular, which are readily available with a wide range of emissions are a major class of NPs used in biological detection due to their favourable photophysical properties [4]. InSb was also designed for mid-infrared plasmonics [40]. In practice, the proximity of the excitation energy of semiconductor NPs and the plasmon exciton energy for metal NPs offers the opportunity to produce nanocomposite materials in which excitation of the semiconductor leads to rapid charge injection into the metal. In a metal-semiconductor thin film diode experiment, the large enhancement in electromagnetic field was observed due to surface plasmon resonance of NPs [37]. The plasmonic effect of the metal-semiconductor nanocomposites interface provided

light trapping effect to allow more plasmon generation. As a result, it enhanced the resonance angle shift and thus the SPR sensing.

23.3.1 Theory for Optical Properties of Core–Shell NP System

The optical properties of core–shell metal-semiconductor nanocomposite are governed by Maxwell Garnett's (MG) theory when a metal NP embedded in a host matrix is subjected to an average polarisation field due to both the matrix as well as the surrounding NPs [23]. According to Drude model, the frequency-dependent complex dielectric function may be written as:

$$\varepsilon(\omega) = \varepsilon^{\infty} - \frac{\omega_p^2}{\omega(\omega + i\omega_d)} \tag{23.3}$$

where ε^{∞} is the high-frequency dielectric function, while ω_p and ω_d are the bulk plasma frequency and damping frequency, respectively. These are given by

$$\omega_p^2 = \frac{Ne^2}{m\varepsilon_0} \tag{23.4}$$

and,

$$\omega_d = \frac{v_f}{R_{bulk}} \tag{23.5}$$

where N represents the concentration of free electrons; m and e represent the effective mass and the charge of the electron. R_{bulk} represents the mean free path of the conduction electrons, and v_f represents the velocity of the electrons at the Fermi energy.

When the particle size, R, is smaller than the mean free path in the bulk metal, conduction electrons are additionally scattered by the surface, and the mean free path, R_{eff}, becomes size-dependent with

$$\frac{1}{R_{eff}} = \frac{1}{R} + \frac{1}{R_{bulk}} \tag{23.6}$$

Hence, the size dependence of damping frequency is given by

$$\omega_d(R) = \omega_d(\text{bulk}) + \frac{v_f}{R} \tag{23.7}$$

Thus, Eq. (23.3) together with Eqs. (23.4)–(23.7) completely represents the size-dependent dielectric function of a metal particle even down to a size of 2 nm. According to MG theory, the effective dielectric function (ε_{av}) of a composite consisting of high-volume-fraction metal NPs isotropically dispersed in a medium is given by the expression

$$\varepsilon_{av} = \varepsilon_m \left(1 + \frac{3\phi\beta}{1-\phi\beta} \right), \text{ where} \tag{23.8}$$

$$\beta = \frac{\varepsilon - \varepsilon_m}{\varepsilon + 2\varepsilon_m} \tag{23.9}$$

and ϕ is the volume fraction of the embedded particles and ε_m is the dielectric function of the host semiconductor material in which the metal particles are embedded. Some of the compound semiconductor materials, which are commonly used in core–shell nanostructures with different semiconductor materials, are CdS, CdSe, PbS and ZnO. The dispersion relation (i.e. the variation of dielectric constant εm with wavelength) for all the four semiconductor materials CdS [74], CdSe [7], PbS [97] and ZnO [10] are available in the related literature.

Usually, MG theory is most appropriate for small spherical NPs (e.g. gold or silver) isotropically distributed within a continuous matrix. The net effect is the creation of a dense matrix of the host material containing mono-disperse metal NPs with known dielectric properties, embedded at a constant, uniform distance from one another. Further, the MG equations deal with the metal volume fraction, so one is still required to specify how the NPs pack within the films. If one assumes that the metal NPs are closely packed, and there is a geometric fcc lattice packing, the volume fraction of the spheres is 0.74 of the total film volume, and the volume fraction of metal particles may be given by Ung et al. [77]

$$\phi = \frac{0.74R^3}{\left(R + R_{host}\right)^3} \tag{23.10}$$

where R_{host}, in the present case, represents the semiconductor shell thickness.

Semiconductor QDs have emerged as fluorescence signal amplifiers to enhance plasmonic biosensors' luminescence signals. QDs-based SPR biosensors can be applied in faster, real-time detection and identification of microbial toxins and to study the interaction of microorganisms with different pathogenic microflora or other molecular species. The inherent ultrahigh RI sensitivity of semiconductor plasmonic materials has been widely explored to detect a quantifiable optical signal corresponding to the RI change of the bio-analytes in which the biological recognition events occurred.

SPR biosensor showed promising results to detect foodborne pathogens related to the processing of poultry, milk and leafy vegetables [8, 38, 48, 75]. A sensitivity as high as 1×10^6 CFU/mL for *Salmonella typhimurium* detection was achieved.

Initial results show that applying NPs mixture with a secondary antibody or a gold-conjugated antibody increased the detection limit. Also, for its application in pathogenic bacteria monitoring, it has the potential to differentiate the pathogens, such as human pathogens *Pseudomonas aeruginosa*, *Brucella* spp. and *Serratia* spp.; and some animal pathogens such as *Photobacterium damselae* and *Aeromonas salmonicida* [48]. The recent study visualised rapid detection and characteristic-specific binding kinetics of full-length tail protein by transmission electron microscopy (TEM). A protein was functionalised on SPR biosensor and then employed for bacterial capture using microagglutination assays [32]. In another study, the plasmo-electronic effect of gold triangular nanoprisms (AuTNPs) enhanced the existing LSPR properties for sensing performances. Hati et al. [29] and his co-workers have designed a nanoplasmonic biosensor design for ultrasensitive, precise and programmable detection of microRNAs and proteins at attomolar concentrations in standard human plasma and urine samples femtomolar concentrations from bladder cancer patient plasma and urine. The solid-state structure comprises the light-induced reversible conformational change of spiropyran (SP)-merocyanine (MC) covalently attached to Au TNPs via alkylthiolate self-assembled monolayers (SAM) to produce a large LSPR response (∼24 nm).

Monitoring the change of a biomarker in real-time allows for identifying the susceptibility to different therapies and interactive optimisation of medical treatments with reduced time and costs compared to clinical validation of therapies. Different protein biomarkers are correlated with the presence of pathogenic processes and diseases. Usually, the performance of a new optical fibre biosensor is evaluated by direct binding model assays. According to the literature, the most standardised biological measurements involving the detection of bioreceptors-analyte complexes are IgG/anti-IgG, streptavidin/biotin and BSA/anti-BSA. They are normally chosen because of their low price, ease of handling, availability and widely-studied binding and immobilisation process. Once the adequate performance of the biosensor is proved, the biomarkers associated with specific pathologies are employed to identify a specific use for the biosensor.

Another important application domain of biosensors is the detection of nucleic acids, which are employed as biomarkers with diverse applications, including diagnosis, prognosis and selection of targeted therapies. Currently, publications on the wavelength-based optical fibre biosensors for nucleic acids are limited, but some research evidences the scientific community's interest in the topic. The most sensitive optical structure among the different fibre gratings optical platforms used to detect specific sequences of DNA was DTP-LPFG (1359 nm/RIU), which reported the lowest LOD: 4 nM (~18.4 ng/mL) of DNA [15]. The selection of appropriate plasmonic material is crucial for good sensing performance from PCF-SPR sensors. Recent researches show that some alloys can also be potential candidates as plasmonic materials for their remarkable plasmonic characteristics. To investigate the sensing performance of the SPR sensor, gold, silver and copper as noble plasmonic materials and gold-silver, gold-silver and copper-zinc as alloys have been selected. The obtained results reported that the sensor shows maximum amplitude sensitivity (AS) of 9759.00 RIU^{-1} and figure of merit (FOM) of 923.07 RIU^{-1} when the silver

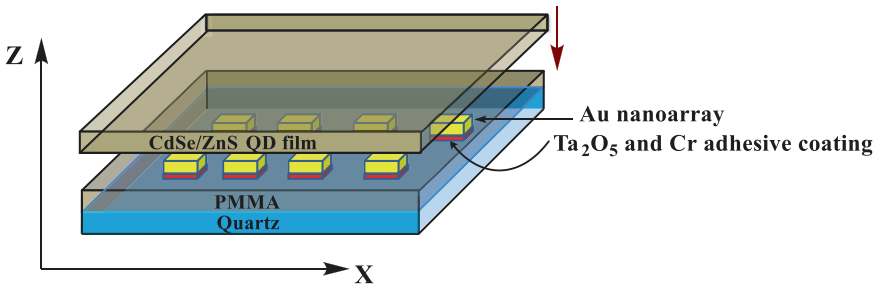

Fig. 23.6 3D diagram to illustrate the CdSe/ZnS quantum dots-based biosensing device on the coupling of exciton and LSPR on the surface of plasmonic nanoarrays coated with a spacer layer of PMMA

coating is used. Moreover, the reported sensor shows maximum spectral sensitivity (SS) of 26,000 nmRIU^{-1} and a resolution of 3.84 × 10^{-6} with copper-zinc alloy. Such sensor probe can be an impressive appliance for the identification of organic substances, biological fluids and samples [64].

Wang et al. [84] have reported LSPR-induced emission enhancement from CdSe/ZnS QDs near well-engineered Au TNPs through a high-performance exciton LSPR coupling system with a versatile Ta_2O_5 layer (Fig. 23.6).

By the combination of the matching conditions and a low extinction coefficient with minimal damping absorption of the Ta_2O_5 layer in the system, stronger LSPR is induced by the efficient coupling between QDs and Au TNPs and efficiently scattering into the far-field without damping. The plasmon-enhanced emission from QDs with a high PL enhancement factor was achieved by the coupling of excitons and LSPRs. It can be observed that the proposed design concept and method with greatly enhanced light-matter interactions will open up avenues toward actual applications of LSPR-based fluorescence enhancement in biomedicine and optoelectronic devices.

23.4 SPR-Enhanced Optical Gas Sensors Based on II–VI Semiconductor QDs

Certain gas molecules and volatile organic compounds (VOCs) are considered to be highly harmful and toxic to human health as well as the natural ecosystem [88]. Formaldehyde and benzene are well-known carcinogenic substances that have a high potential for adverse effects on the human respiratory and immune systems [62, 92]. Furthermore, organic compounds such as dioxins, acetone, nitrogen, ethyl alcohol, n-hexane, chlorobenzene, o-xylene and toluene have a prolonged effect on human health and showed high responsivity when exposed to the environment [50]. Concerning the potential hazards of VOCs and even their small leakage in hostile environments may cause serious respiratory disorders and chronic skin diseases.

Therefore, effective VOCs monitoring methods are greatly in demand for measuring and monitoring the atmospheric environment and human well-being and health surveillance. Present high-sensitive analytical methods, such as high-performance liquid chromatography (HPLC) [26], gas chromatography (GC) [61] and spectrophotometry [76] have been used to detect the ultra-low concentrations of VOCs, which are based on expensive set-up and rigorous experimental conditions [20, 79].

Carbon-based fluorescent nanomaterials (e.g. graphene QDs) have been studied empathetically to detect toxic gas leakages that can be used as intelligent functionalised photonic materials in the field of gas sensing and biosensing [42, 44]. However, the surface functionalisation of graphene QDs needed further improvement in order to enhance their fluorescence performance in an aqueous environment. Furthermore, their potential use in the detection of gas molecules is still largely untapped due to chemical and electrochemical stability in a small potential window. As a consequence, their low stability remains the biggest challenge for practical gas detection applications [81, 82]. These disadvantages have shifted the focus of the scientific community to synthesise semiconductor-based photonic NPs with the smallest size.

It is known that conductometric devices based on nanostructured semiconductor materials, such as metal oxides and II–VI compounds, make it possible to control the appearance and determine the concentration of toxic gases and VOCs in the atmosphere. The choice of semiconductor materials for the detection of a specific gas is determined by the influence of the interaction of its superficial active surface sides created by chemisorbed O^-, O^{2-}, H^+ and OH-ions with molecules of detected gas on their electrical conductivity [49]. The choice of nanostructured semiconductors for gas sensing is due to the reversibility of the processes of interaction with the detected gases and high sensitivity. At the same time, it was shown that as gas molecules are absorbed onto the metal oxide NP surface, changes in the dielectric constant occur that cause changes in the RI. This means that surface plasmon structures based on nanostructured semiconductors can also be used to detect toxic gases and VOCs in the atmosphere. The experiment confirmed this assumption.

Recently, a research group has proposed SPR-based formaldehyde sensor with very low (~0.5 ppm) detection range by depositing the mixture of amino-modified CdSe@ZnS QDs, fumed silica and gold NPs on the surface of the silica sphere. Under the optimisation conditions, the fluorescence intensity showed significant quenching to gaseous formaldehyde (~1.0 ppm) with a short response time, as seen in Fig. 23.7 [92]. SPRbased gas sensor emerged as an excellent and precautionary sensory technique for the identification and qualitative determination of VOCs concentration. It is worth mentioning that the SPR gas sensor showed accurate sensitivity, high stability and reproducibility with good recoverability in a short response.

Wu et al. [91] also embedded semiconductor QDs in the SPR configuration and found that this device can be considered as rapid, sensitive and convenient gas sensor. The nanocomposite scaffold consists of CdSe-CdS core–shell semiconductor quantum rods, Ag NPs and poly(methyl methacrylate) (PMMA) nanofibres (Fig. 23.8).

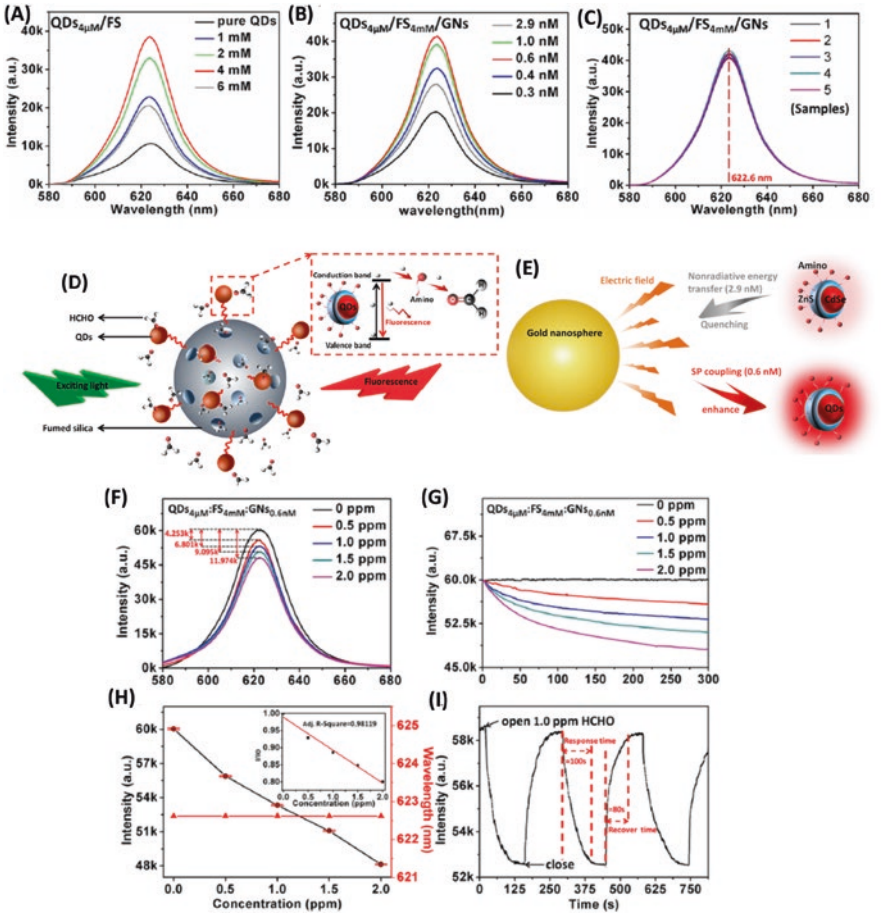

Fig. 23.7 (**a**) Fluorescence intensities of sensing films with different concentrations of fumed silica (FS) solutions together with that of pure QDs. (**b**) Fluorescence intensities of sensing films with different concentrations of gold NP (GN) solutions based on $QDs_{4\mu M}/FS_{4mM}$. (**c**) Fluorescence intensities and wavelengths of different samples fabricated under the same conditions. (**d**) Fluorescence quenching mechanism (**e**) The mechanism of influence of gold nanoshpere on the quenching and enhancement of fluorescence (**f**) Sensing performance of quantum dot-based PEF sensors under optimization conditions ($QDs_{4\mu M}/FS_{4mM}/GNs_{0.6nM}$). (**g**) Fluorescence intensities of sensing films after injecting different concentrations of gaseous formaldehyde for 500 s. (**h**) Variation of fluorescence intensities in different concentrations of gaseous formaldehyde within 500 s. The relationship between the fluorescence intensity and the formaldehyde concentration. The inset shows a calibration plot of the presented sensor for formaldehyde over the range of 0.5–2.0 ppm (n = 5, Adj. R^2:0.98119). (**i**) Response-recovery properties of sensing devices at 1.0 ppm concentration of formaldehyde. (Reprinted with permission from Xue et al. [92]. Copyright 2020: American Chemical Society)

CdSe-CdS/Ag/PMMA-based sensors showed versatile sensitivity below the lowest explosion limits. In fact, it reached a non-selective detection threshold of 500 ppm for chlorobenzene and 100 ppm for butanol [91]. Mishra et al. [51] employed an LMR-based hydrogen gas sensor by coating an ITO (In_2O_3+ SnO_2)

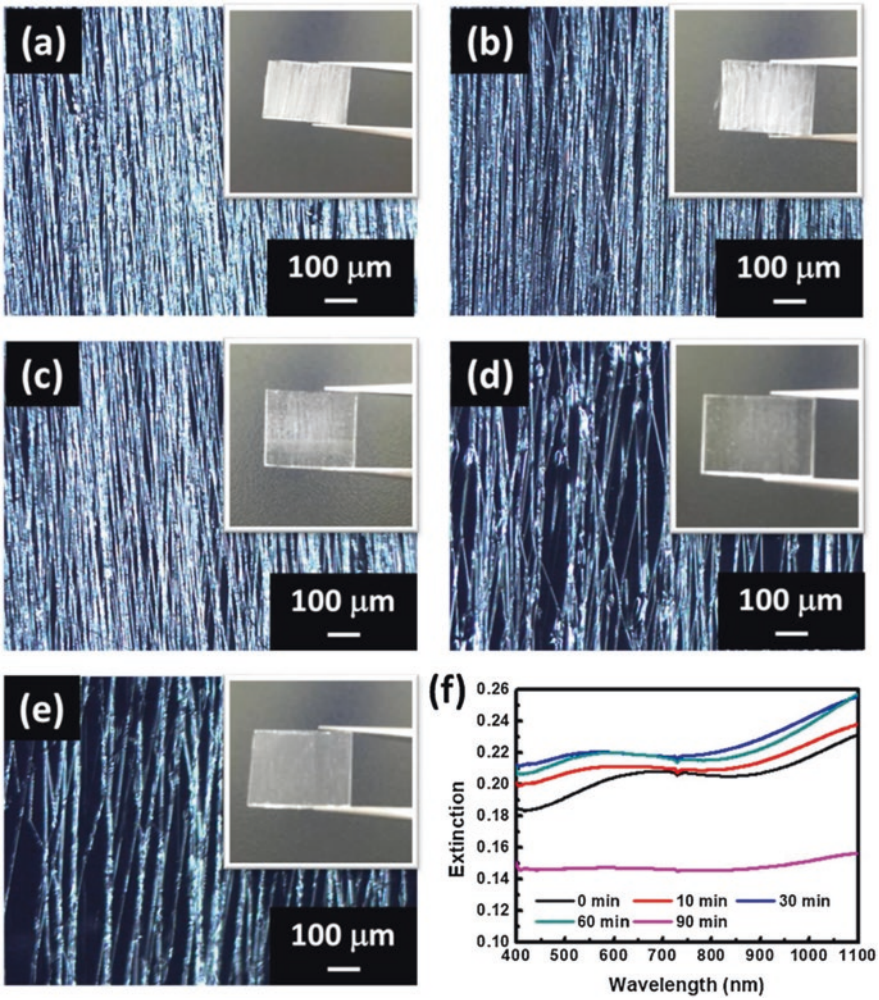

Fig. 23.8 The optical images of CdSe-CdS/Ag/PMMA composite scaffolds treated with UV-ozone etching after (**a**) 0 min, (**b**) 10 min, (**c**) 30 min, (**d**) 60 min and (**e**) 90 min. The insets are the photographs of each sensing chip. (**f**) The extinction spectra of CdSe-CdS/Ag/PMMA composite scaffolds with various etching time. (Reprinted with permission from Wu et al. [91]. Copyright 2020: Elsevier)

thin film on the core of an optical fibre [52]. The same researcher later reposted a highly sensitive SPR-based ammonia gas sensor designed using ITO and polyaniline thin film. Further, an LSPR gas detection system has been developed, in which evaporated gold island films have been coated with polymer polystyrene sulphuric acid and polystyrene. These polymers swell and/or shrink when exposed to the various gases used (chloroform, water vapour, etc.), which affects the local RI and causes an intense peak of LSPR [35].

23.5 SPR-Based Biosensors Functionalised with II–VI Semiconductor QDs

The direct band-gap plasmonic semiconductor nanomaterials (II–VI: CdS, CdSe, CdTe, etc.; III–V: InP, InAs, etc.; IV–VI: PbSe, etc.) are widely classified for changes to RI variations at the sensor surface. The changes in RI practically offer the potential of measuring low levels of biological signals adjutant to the metallic NP boundaries. Such NPs and their combination with plasmonic semiconductors have been extensively modified with the linker molecules to couple with biomolecules for developing plasmonic biosensors (Fig. 23.9). Interestingly, gold NP islands have shown exceptional LSPR properties, which make them unique colorimetric biosensors [18]. Their high optical excitation coefficient, broad absorption spectrum, fluorescence quenching and catalytic efficacy showed a non-radiative energy transfer process, called the fluorescence resonance energy transfer (FRET) phenomenon. FRET is another method to identify the proteins or histone modifications associated with a specific DNA sequence [69].

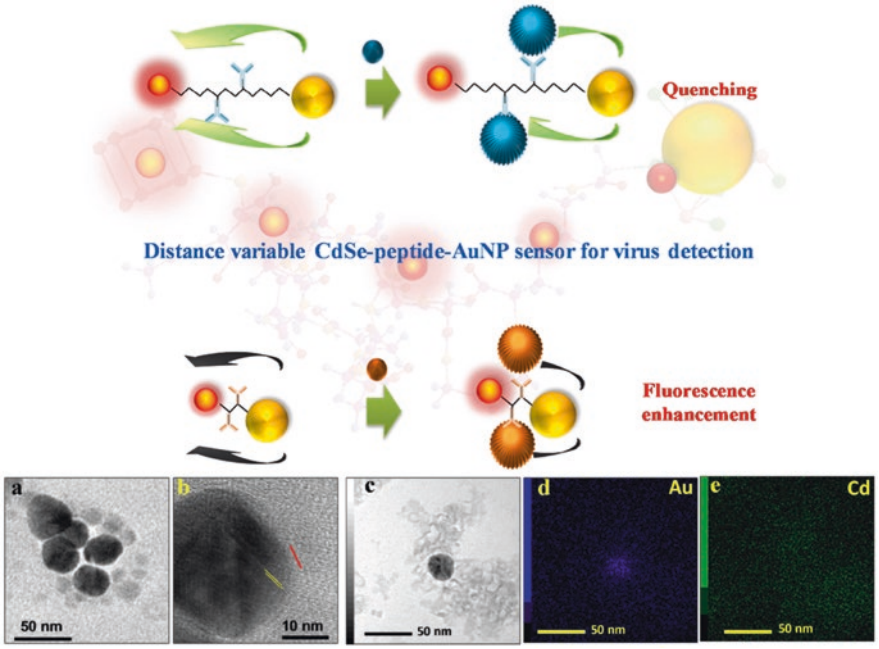

Fig. 23.9 Virus detection with the sensor probe varying the peptide length: schematic illustration for the virus sensing using CdSe QD-peptide-AuNP system for two modes of detection and characterisations of CdSe QD-peptide-AuNP nanoconjugate: (**a**) TEM image (**b**) HRTEM image of CdSe QD-peptide-AuNP, showing their own fringes, (**c**–**e**) STEM mapping of CdSe QD-peptide-AuNP with Cd and Au. (Reprinted with permission from Chowdhury et al. [18]. Copyright 2020: Elsevier)

Early-stage diagnosis and appropriate treatment are vital challenges in the fight against cancer. As an alternative tool for conventional options, SPR-based label-free detection of cancer biomarkers in real-time with high sensitivity (picomolar level) is comparable to that of single-colour and dual-colour labelling approaches. The plasmon resonance characteristics of QD NPs and their associated electromagnetic field enhancement produced by LSPR excitation have made feasible the design of biosensors for the exosome quantification in liquid biopsies for cancer diagnosis. The considerably enhanced response and visual detection of protein binding may demonstrate using gold NPs stabilised with the linker-modified molecules. LSPR colorimetric sensors based on the aggregation of NPs may provide high sensitivities and functional designs.

The stability of plasmonic NP assemblies can be modulated through covalent or non-covalent interactions (i.e. electrostatic interactions, hydrophobic forces, hydrogen linkage and specific biological linkage) and depend greatly on external conditions such as temperature, pH and buffer. Au NPs are functionalised by the non-covalent bio-conjugated system with a panel of DNA aptamers, which are able to bind the exosome surface proteins with high specificity and affinity. Their individual appearance reflected in distinctive colours as a consequence of NP aggregation (from red to blue) following the specific binding between the aptamers and cell-surface proteins (Fig. 23.10). These colorimetric changes are responsible for generating patterns to identify the multiple proteins on the exosome surface, which can be further implemented for cancer diagnosis [34].

LSPR biosensors can be designed for solution-phase or surface-bound sensors and can result in a spectral change in absorption/extinction or scattering and even colour variation of plasmonic NP solutions. Solution-based biosensors are much more attractive due to the less complexity of the measurement and of the assay analysis [85]. Strong emphasis has been given to the colloidal NPs in complex liquid medium because of the formation of a protein corona and ionic potency of the

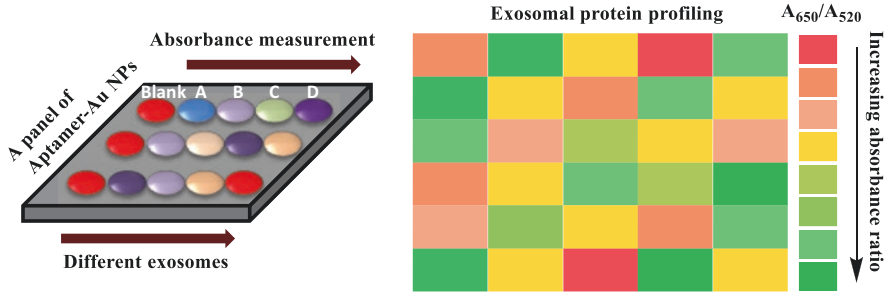

Fig. 23.10 A coat of many colours: A gold NP/aptamer biosensor (AuNP/AptX) provides a colorimetric platform for rapid and multiplexed protein analysis of exosomes. (Adapted with permission from Jiang et al. [34]. Copyright 2017: Wiley)

biofluids. In combination with a unique set of plasmonic properties of LSPR nanomaterials, the hydrophobic interactions can be potentially used in both biosensing and nanomedicine. The impact of complex liquid media on LSPR sensors can be condensed by functionalising the layers, biological scaffolds and particle diameter, but yet remains an issue to believe. Dilution of the media can also be an option to minimise the impacts related to the biofluid, as shown for sensing real samples. Solution-based LSPR can also serve to conquer the response of an ELISA assay for real samples.

On the other side, surface-bound LSPR sensors are fabricated by immobilisation of NPs on a solid substrate to alleviate the concerns of the colloidal stability of NPs in liquid media solution. This configuration is also simpler to multiplex on-chip and to integrate with microfluidics. The field of integrated plasmonic devices is gaining a lot of attention recently. Typical bioreceptors include, in general, antibodies, enzymes, proteins, aptamers, cells, or microorganisms. They are specially designed to detect other target molecules, also known as "analytes" or "biomarkers". Once deposited on the transducer substrate, these biological interactions transform into measurable variables and simulate them into optical, electrical, mechanical, or acoustic signals that can be further treated [73]. Finally, the bio-functionalised interface is the middle layer. It consists of one or more layer-by-layer (LbL) that binds the bioreceptors to the substrate using nanotechnology-based manufacturing techniques.

Many materials other than pure metals (typical of SPRs) can induce LMRs. Thus, significant progress has been reported on LMRs with metal oxides, polymer coatings; LbL-coated structures and considered an almost unavoidable component in the majority of combining plasmonic materials or even immunosensors consisting of multilayer of polymers and antibodies [68]. Furthermore, SPR biosensing surfaces can be functionalised by thin polymer films to which antibodies are coupled through amino groups [54]. Protein contact printing was considered for spatially controlled binding of bovine serum albumin (BSA) and dinitrophenylated BSA to adjacent reference and signal channels of a dual-channel SPR sensor [46]. Nano-range biomolecules can be immobilised on the surfaces of gold SPR sensors by forming a streptavidine layer on a gold surface followed by biotinylated DNA attachment [86]. A multi-step surface modification based on alkanethiol SAM was also used to attach DNA to gold surfaces [12]. Then, later, biomimetic materials made from micro-contact imprinting techniques for the detection of urinary tract pathogens have been exploited in SPR biosensors [56].

Novel semiconductor nanostructures for LSPR sensing are frequently reported for optimising the sensitivity of sensors. The advantage of a colloidal NP-based LSPR sensor is the possibility of naked-eye detection from aggregation assays, NP etching, or growth mechanism, such as for the detection of glucose [33]. These possibilities are highly promising and the use of gold NPs in microfluidic-based biosensing for point-of-care applications has attracted a lot of attention. LSPR biosensors can be designed for solution-phase or surface-bound sensors. Solution-based biosensors are interesting due to the simplicity of the measurement and of the

assay. Biomolecule-attached metal NPs are the most popular probes for easy separation by centrifugation and can be readily assembled with thiolated molecules. The single-crystalline Au islands furnished the possibility of effective separation of the surface-plasmon bands of the islands and the bound NPs. LSPR provides a plasmon resonance in a broader optical window, enhances sensitivity, facilitates integration into a simple device, comprises easy surface chemistry, and is relatively economical to fabricate.

Plasmonic nanostructures are either prepared from colloidal synthesis or with nanofabrication techniques. Nanofabricated plasmonic structures can reach high FOM, and, thus, their performance can exceed other SPR sensing platforms but may be very costly and complex to fabricate. Hence, the fabrication of LSPR NPs on a solid substrate is widely employed to alleviate some of the issues, such as stability and ease of integration with microfluidic. Placing an NP on a colloidal substrate affects the optical properties and sensitivity. But, when it comes to the RI sensitivity, FOM and RI resolution are bulk properties; the penetration depth is directly associated with the sensitivity of the device to a binding event, which straightly influences the RI shift from the detection of a molecule.

Generally, the penetration depth is expected to be relatively small but even greater than the molecules to be detected to ensure that the binding events result in a significant change in the wavelength or resonance angle of the plasmon. A drawback of the SPR is the requirement of sufficient quantities of ligand which is successfully connected to the surface of the sensor chip. Moreover, this ligand must be sufficiently robust to withstand several regeneration cycles. There is currently a large heterogeneity in nanostructures used for SPR sensing, and therefore focus needed to be placed on identifying the best anisotropic or pronged colloidal nanostructures and optimising their synthesis to achieve highly reproducible fabrication, as well as identifying 2D nanofabricated surfaces that are relatively simple to fabricate and of high sensitivity. This constitutes the major challenge of plasmonic nanomaterials, as methods for classical SPR sensing should be translated with relatively few obstacles [78]. The scope of QDs synthesis is very broad and cannot be fully explored from a specific application perspective, so only colloidal stability is the main concern. Colloidal synthesis facilitates the advantage of simplicity and cost-effective fabrication, but colloidal-based sensors often suffer from reproducibility in synthesis and usually have a lower FOM.

23.6 Conclusions and Future Directions

Semiconducting nanostructure-based SPR sensor is a promising approach for making a progression in advanced biosensing applications. Their specificity and active surface feature advantageously for light entrapment within a smaller region. Quantum dot and metal oxide-based gas sensing devices are expanding their infrared bandwidth utilisation. The discussion projected on the metal-semiconductor nanocomposites provides deep insights into the important aspects, such as surface

features, fabrication, sensitivity, label-free detection and in-vivo adaptation. The sensitivity to the detection of biomolecules and target molecules in the complex fluids described in the chapter required increased miniaturisation and user-friendly interface design. In the forthcoming era of printable devices, semiconductor materials will gain significant foresight in lithographic research. The flexibility of semiconductor film can result in portable devices with great potential for health monitoring and toxic gas leakages. Thus, the futuristic sensory device would be reusable, easy to operate, simple to functionalised with the recognition element and replace in terms of hardware and software.

Acknowledgements Anuj K. Sharma gratefully acknowledges the sponsored research project grants "03(1441)/18/EMR-II" and "CRG/2019/002636" funded by the Council of Scientific & Industrial Research (India) and the Science & Engineering Research Board (India), respectively.

References

1. Agrawal A, Cho SH, Zandi O, Ghosh S, Johns RW, Milliron DJ. Localized surface Plasmon resonance in semiconductor nanocrystals. Chem Rev. 2018;118(6):3121–207. https://doi.org/10.1021/acs.chemrev.7b00613.
2. Akgönüllü S, Yavuz H, Denizli A. SPR nanosensor based on molecularly imprinted polymer film with gold NPs for sensitive detection of aflatoxin B1. Talanta. 2020;219:121219. https://doi.org/10.1016/j.talanta.2020.121219.
3. Ali MA, Srivastava S, Pandey MK, Agrawal VV, John R, Malhotra BD. Protein-conjugated quantum dots interface: binding kinetics and label-free lipid detection. Anal Chem. 2014;86(3):1710–8. https://doi.org/10.1021/ac403543g.
4. Aubret A, Pillonnet A, Houel J, Dujardin C, Kulzer F. CdSe/ZnS quantum dots as sensors for the local RI. Nanoscale. 2016;8(4):2317–25. https://doi.org/10.1039/c5nr06998j.
5. Barho FB, Gonzalez-Posada F, Milla-Rodrigo M-J, Bomers M, Cerutti L, Taliercio T. All-semiconductor plasmonic gratings for biosensing applications in the mid-infrared spectral range. Opt Express. 2016;24(14):16175. https://doi.org/10.1364/oe.24.016175.
6. Bhalla N, Pan Y, Yang Z, Payam AF. Opportunities and challenges for biosensors and nanoscale analytical tools for pandemics: COVID-19. ACS Nano. 2020;14(7):7783–807. https://doi.org/10.1021/acsnano.0c04421.
7. Bhar GC. RI interpolation in phase-matching. Appl Opt. 1976;15(2):305_1. https://doi.org/10.1364/ao.15.0305_1.
8. Bokken GCAM, Corbee RJ, Van Knapen F, Bergwerff AA. Immunochemical detection of Salmonella group B, D and E using an optical surface plasmon resonance biosensor. FEMS Microbiol Lett. 2003;222(1):75–82. https://doi.org/10.1016/S0378-1097(03)00250-7.
9. Boltasseva A, Atwater HA. Low-loss plasmonic metamaterials. Science. 2011;331(6015):290–1. https://doi.org/10.1126/science.1198258.
10. Bond WL. Measurement of the refractive indices of several crystals. J Appl Phys. 1965;36(5):1674–7. https://doi.org/10.1063/1.1703106.
11. Breault-Turcot J, Chaurand P, Masson JF. Unravelling nonspecific adsorption of complex protein mixture on surfaces with SPR and MS. Anal Chem. 2014;86(19):9612–9. https://doi.org/10.1021/ac502077b.
12. Brockman JM, Frutos AG, Corn RM. A multistep chemical modification procedure to create dna arrays on gold surfaces for the study of protein-DNA interactions with surface plasmon resonance imaging. J Am Chem Soc. 1999;121(35):8044–51. https://doi.org/10.1021/ja991608e.

13. Cao Y, Griffith B, Bhomkar P, Wishart DS, McDermott MT. Functionalized gold NP-enhanced competitive assay for sensitive small-molecule metabolite detection using surface plasmon resonance. Analyst. 2018;143(1):289–96. https://doi.org/10.1039/c7an01680h.
14. Chang CC. Recent advancements in aptamer-based surface plasmon resonance biosensing strategies. Biosensors. 2021;11(7). https://doi.org/10.3390/bios11070233.
15. Chen Liu XC. EDC-mediated oligonucleotide immobilization on a long period grating optical biosensor. J Biosens Bioelectron. 2015;6(2):1000173. https://doi.org/10.4172/2155-6210.1000173.
16. Cheng XR, Hau BYH, Endo T, Kerman K. Au NP-modified DNA sensor based on simultaneous electrochemical impedance spectroscopy and localized surface plasmon resonance. Biosens Bioelectron. 2014;53:513–8. https://doi.org/10.1016/j.bios.2013.10.003.
17. Chiang HP, Chen CW, Wu JJ, Li HL, Lin TY, Sánchez EJ, Leung PT. Effects of temperature on the surface plasmon resonance at a metal-semiconductor interface. Thin Solid Films. 2007;515(17):6953–61. https://doi.org/10.1016/j.tsf.2007.02.034.
18. Chowdhury AD, Nasrin F, Gangopadhyay R, Ganganboina AB, Takemura K, Kozaki I, et al. Controlling distance, size and concentration of nanoconjugates for optimized LSPR based biosensors. Biosens Bioelectron. 2020;170:112657. https://doi.org/10.1016/j.bios.2020.112657.
19. Dahlman CJ, Agrawal A, Staller CM, Adair J, Milliron DJ. Anisotropic origins of localized surface plasmon resonance in n-type Anatase TiO_2 nanocrystals. Chem Mater. 2019;31(2):502–11. https://doi.org/10.1021/acs.chemmater.8b04519.
20. Descamps MN, Bordy T, Hue J, Mariano S, Nonglaton G, Schultz E, et al. Real-time detection of formaldehyde by a fluorescence-based sensor. Procedia Eng. 2010;5:1009–12. https://doi.org/10.1016/j.proeng.2010.09.280.
21. Ermini ML, Song XC, Špringer T, Homola J. Peptide functionalization of gold NPs for the detection of carcinoembryonic antigen in blood plasma via SPR-based biosensor. Front Chem. 2019;7:40. https://doi.org/10.3389/fchem.2019.00040.
22. Fasoli JB, Corn RM. Surface enzyme chemistries for ultrasensitive microarray biosensing with SPR imaging. Langmuir. 2015;31(35):9527–36. https://doi.org/10.1021/la504797z.
23. Garnett JCM. XII. Colours in metal glasses and in metallic films. Philos Trans R Soc London, Series A. 1904;203(359–371):385–420. https://doi.org/10.1098/rsta.1904.0024.
24. Ghrera AS, Pandey MK, Malhotra BD. Quantum dot monolayer for surface plasmon resonance signal enhancement and DNA hybridization detection. Biosens Bioelectron. 2016;80:477–82. https://doi.org/10.1016/j.bios.2016.02.013.
25. Giannini V, Vecchi G, Gómez Rivas J. Lighting up multipolar surface plasmon polaritons by collective resonances in arrays of nanoantennas. Phys Rev Lett. 2010;105(26):266801. https://doi.org/10.1103/PhysRevLett.105.266801.
26. Gil RL, Amorim CG, Montenegro MCBSM, Araújo AN. HPLC-potentiometric method for determination of biogenic amines in alcoholic beverages: a reliable approach for food quality control. Food Chem. 2022;372:131288. https://doi.org/10.1016/j.foodchem.2021.131288.
27. Haes AJ, Van Duyne RP. A nanoscale optical biosensor: sensitivity and selectivity of an approach based on the localized surface plasmon resonance spectroscopy of triangular silver NPs. J Am Chem Soc. 2002;124(35):10596–604. https://doi.org/10.1021/ja020393x.
28. Hasan MR, Akter S, Rifat AA, Rana S, Ahmed K, Ahmed R, Subbaraman H, Abbott D. Spiral photonic crystal fiber-based dual-polarized surface plasmon resonance biosensor. IEEE Sensors J. 2018;18(1):133–40. https://doi.org/10.1109/JSEN.2017.2769720.
29. Hati S, Langlais SR, Masterson AN, Liyanage T, Muhoberac BB, Kaimakliotis H, Johnson M, Sardar R. Photoswitchable machine-engineered plasmonic nanosystem with high optical response for ultrasensitive detection of microRNAs and proteins adaptively. Anal Chem. 2021;93(41):13935–44. https://doi.org/10.1021/acs.analchem.1c02990.
30. Hinman SS, McKeating KS, Cheng Q. Surface plasmon resonance: material and interface design for universal accessibility. Anal Chem. 2018;90(1):19–39. https://doi.org/10.1021/acs.analchem.7b04251.

31. Huang Y, Zhang L, Zhang H, Li Y, Liu L, Chen Y, Qiu X, Yu D. Development of a portable SPR sensor for nucleic acid detection. Micromachines. 2020;11(5). https://doi.org/10.3390/mi11050526.
32. Hyeon SH, Lim WK, Shin HJ. Novel surface plasmon resonance biosensor that uses full-length Det7 phage tail protein for rapid and selective detection of Salmonella enterica serovar Typhimurium. Biotechnol Appl Biochem. 2021;68(1):5–12. https://doi.org/10.1002/bab.1883.
33. Jiang Y, Zhao H, Lin Y, Zhu N, Ma Y, Mao L. Colorimetric detection of glucose in rat brain using gold NPs. Angew Chem Int Ed. 2010;49(28):4800–4. https://doi.org/10.1002/anie.201001057.
34. Jiang Y, Shi M, Liu Y, Wan S, Cui C, Zhang L, Tan W. Aptamer/AuNP biosensor for colorimetric profiling of exosomal proteins. Angew Chem. 2017;129(39):12078–82. https://doi.org/10.1002/ange.201703807.
35. Karakouz T, Vaskevich A, Rubinstein I. Polymer-coated gold island films as localized plasmon transducers for gas sensing. J Phys Chem B. 2008;112(46):14530–8. https://doi.org/10.1021/jp804829t.
36. Kluková L, Bertok T, Kasák P, Tkac J. Nanoscale-controlled architecture for the development of ultrasensitive lectin biosensors applicable in glycomics. Anal Methods. 2014;6(14):4922–31. https://doi.org/10.1039/c4ay00495g.
37. Konda RB, Mundle R, Mustafa H, Bamiduro O, Pradhan AK, Roy UN, et al. Surface plasmon excitation via Au NPs in n-CdSe/p-Si heterojunction diodes. Appl Phys Lett. 2007;91(19):191111. https://doi.org/10.1063/1.2807277.
38. Lan YB, Wang SZ, Yin YG, Hoffmann WC, Zheng XZ. Using a surface plasmon resonance biosensor for rapid detection of salmonella typhimurium in chicken carcass. J Bionic Eng. 2008;5(3):239–46. https://doi.org/10.1016/S1672-6529(08)60030-X.
39. Law S, Yu L, Wasserman D. Epitaxial growth of engineered metals for mid-infrared plasmonics. J Vac Sci Technol B, Nanotechnol Microelectron. 2013;31(3):03C121. https://doi.org/10.1116/1.4797487.
40. Law S, Liu R, Wasserman D. Doped semiconductors with band-edge plasma frequencies. J Vac Sci Technol B, Nanotechnol Microelectron. 2014;32(5):052601. https://doi.org/10.1116/1.4891170.
41. Li D, Ning CZ. All-semiconductor active plasmonic system in mid-infrared wavelengths. Opt Express. 2011;19(15):14594. https://doi.org/10.1364/oe.19.014594.
42. Li Y, Zhao Y, Cheng H, Hu Y, Shi G, Dai L, Qu L. Nitrogen-doped graphene quantum dots with oxygen-rich functional groups. J Am Chem Soc. 2012;134(1):15–8. https://doi.org/10.1021/ja206030c.
43. Li X, Wang M, Zhang B. Equivalent medium theory of layered sphere particle with anisotropic shells. J Quant Spectrosc Radiat Transfer. 2016;179:165–9. https://doi.org/10.1016/j.jqsrt.2016.03.008.
44. Li HJ, Sun X, Xue F, Ou N, Sun BW, Qian DJ, et al. Redox induced fluorescence on-off switching based on nitrogen enriched graphene quantum dots for formaldehyde detection and bioimaging. ACS Sustain Chem Eng. 2018;6(2):1708–16. https://doi.org/10.1021/acssuschemeng.7b02941.
45. Liu G, Qi S, Chen J, Lou Y, Zhao Y, Burda C. Cu-Sb-S ternary semiconductor NP plasmonics. Nano Lett. 2021;21(6):2610–7. https://doi.org/10.1021/acs.nanolett.1c00006.
46. Lu HB, Homola J, Campbell CT, Nenninger GG, Yee SS, Ratner BD. Protein contact printing for a surface plasmon resonance biosensor with on-chip referencing. Sensors Actuators B Chem. 2001;74(1–3):91–9. https://doi.org/10.1016/S0925-4005(00)00716-4.
47. Mauriz E. Recent progress in plasmonic biosensing schemes for virus detection. Sensors (Switzerland). 2020;20(17):1–27. https://doi.org/10.3390/s20174745.
48. Mazumdar SD, Hartmann M, Kämpfer P, Keusgen M. Rapid method for detection of Salmonella in milk by surface plasmon resonance (SPR). Biosens Bioelectron. 2007;22(9–10):2040–6. https://doi.org/10.1016/j.bios.2006.09.004.

49. Mei GS, Susthitha Menon P, Hegde G. ZnO for performance enhancement of surface plasmon resonance biosensor: a review. Mater Res Express. 2020;7(1) https://doi.org/10.1088/2053-1591/ab66a7.
50. Mirzaei A, Leonardi SG, Neri G. Detection of hazardous volatile organic compounds (VOCs) by metal oxide nanostructures-based gas sensors: a review. Ceram Int. 2016;42(14):15119–41. https://doi.org/10.1016/j.ceramint.2016.06.145.
51. Mishra SK, Kumari D, Gupta BD. Surface plasmon resonance based fiber optic ammonia gas sensor using ITO and polyaniline. Sensors Actuators B Chem. 2012;171–172:976–83. https://doi.org/10.1016/j.snb.2012.06.013.
52. Mishra SK, Usha SP, Gupta BD. A lossy mode resonance-based fiber optic hydrogen gas sensor for room temperature using coatings of ITO thin film and NPs. Meas Sci Technol. 2016;27(4):045103. https://doi.org/10.1088/0957-0233/27/4/045103.
53. Naik GV, Shalaev VM, Boltasseva A. Alternative plasmonic materials: beyond gold and silver. Adv Mater. 2013;25(24):3264–94. https://doi.org/10.1002/adma.201205076.
54. Oliverio M, Perotto S, Messina GC, Lovato L, De Angelis F. Chemical functionalization of plasmonic surface biosensors: a tutorial review on issues, strategies, and costs. ACS Appl Mater Interfaces. 2017;9(35):29394–411. https://doi.org/10.1021/acsami.7b01583.
55. Ou H, Cheng T, Zhang Y, Liu J, Ding Y, Zhen J, et al. Surface-adaptive zwitterionic NPs for prolonged blood circulation time and enhanced cellular uptake in tumor cells. Acta Biomater. 2018;65:339–48. https://doi.org/10.1016/j.actbio.2017.10.034.
56. Özgür E, Topçu AA, Yılmaz E, Denizli A. Surface plasmon resonance based biomimetic sensor for urinary tract infections. Talanta. 2020;212:120778. https://doi.org/10.1016/j.talanta.2020.120778.
57. Pereira RMS, Borges J, Smirnov GV, Vaz F, Vasilevskiy MI. Surface plasmon resonance in a metallic NP embedded in a semiconductor matrix: exciton-plasmon coupling. ACS Photon. 2019;6(1):204–10. https://doi.org/10.1021/acsphotonics.8b01430.
58. Qu JH, Dillen A, Saeys W, Lammertyn J, Spasic D. Advancements in SPR biosensing technology: an overview of recent trends in smart layers design, multiplexing concepts, continuous monitoring and in vivo sensing. Anal Chim Acta. 2020;1104:10–27. https://doi.org/10.1016/j.aca.2019.12.067.
59. Raether H, Hohler G, Niekisch EA. Surface plasmons on smooth and rough surfaces and on gratings. In: Raether H, editor. Springer tracts in modern physics, vol. 111. Berlin: Springer; 1988. p. 136. https://doi.org/10.1007/BFb0048317.
60. Saleviter S, Fen YW, Sheh Omar NA, Mustaqim Mohd Daniyal WME, Abdullah J, Mat Zaid MH. Structural and optical studies of cadmium sulfide quantum dot-graphene oxide-chitosan nanocomposite thin film as a novel SPR spectroscopy active layer. J Nanomater. 2018;2018:4324072. https://doi.org/10.1155/2018/4324072.
61. Santos FJ, Galceran MT. Modern developments in gas chromatography-mass spectrometry-based environmental analysis. J Chromatogr A. 2003;1000(1–2):125–51. https://doi.org/10.1016/S0021-9673(03)00305-4.
62. Scharf P, Broering MF, da Rocha GHO, Farsky SHP. Cellular and molecular mechanisms of environmental pollutants on hematopoiesis. Int J Mol Sci. 2020;21(19):1–30. https://doi.org/10.3390/ijms21196996.
63. Shabaninezhad M, Kayani A, Ramakrishna G. Theoretical investigation of optical properties of embedded plasmonic NPs. Chem Phys. 2021;541:111044. https://doi.org/10.1016/j.chemphys.2020.111044.
64. Shafkat A, Reja MI, Miah MJ, Fatema S, Absar R, Akhtar J. Numerical exploration of external sensing scheme based photonic crystal fiber surface plasmonic sensor with different noble plasmonic materials and their alloys. Optik. 2021;231:166418. https://doi.org/10.1016/j.ijleo.2021.166418.
65. Sharma AK, Gupta BD. Metal-semiconductor nanocomposite layer based optical fibre surface plasmon resonance sensor. J Opt A Pure Appl Opt. 2007;9(2):180–5. https://doi.org/10.1088/1464-4258/9/2/011.

66. Sharma AK, Pandey AK, Kaur B. Simulation study on comprehensive sensing enhancement of BlueP/MoS_2 - and BlueP/WS_2 -based fluoride fiber surface plasmon resonance sensors: analysis founded on damping, field, and optical power. Appl Opt. 2019;58(16):4518. https://doi.org/10.1364/ao.58.004518.
67. Singh S, Prajapati YK. TiO_2/gold-graphene hybrid solid core SPR based PCF RI sensor for sensitivity enhancement. Optik. 2020;224:165525. https://doi.org/10.1016/j.ijleo.2020.165525.
68. Socorro-Leránoz AB, Santano D, Del Villar I, Matias IR. Trends in the design of wavelength-based optical fibre biosensors (2008–2018). Biosens Bioelectron. 2019;1:100015. https://doi.org/10.1016/j.biosx.2019.100015.
69. Stryer L. Fluorescence energy transfer as a spectroscopic ruler. Annu Rev Biochem. 1978;47(5):819–46. https://doi.org/10.1146/annurev.bi.47.070178.004131.
70. Tadimety A, Wu Z, Molinski JH, Beckerman R, Jin C, Zhang L, et al. Rational design of on-chip gold plasmonic NPs towards ctDNA screening. Sci Rep. 2021;11(1):1–10. https://doi.org/10.1038/s41598-021-93207-7.
71. Takemura K, Adegoke O, Suzuki T, Park EY. A localized surface plasmon resonance-amplified immunofluorescence biosensor for ultrasensitive and rapid detection of nonstructural protein 1 of Zika virus. PLoS One. 2019;14(1):1–14. https://doi.org/10.1371/journal.pone.0211517.
72. Tandon B, Ghosh S, Milliron DJ. Dopant selection strategy for high-quality factor localized surface plasmon resonance from doped metal oxide nanocrystals. Chem Mater. 2019;31(18):7752–60. https://doi.org/10.1021/acs.chemmater.9b02917.
73. Tang L, Li J. Plasmon-based colorimetric nanosensors for ultrasensitive molecular diagnostics. ACS Sensors. 2017;2(7):857–75. https://doi.org/10.1021/acssensors.7b00282.
74. Tatian B. Fitting refractive-index data with the Sellmeier dispersion formula. Appl Opt. 1984;23(24):4477. https://doi.org/10.1364/ao.23.004477.
75. Taylor AD, Ladd J, Yu Q, Chen S, Homola J, Jiang S. Quantitative and simultaneous detection of four foodborne bacterial pathogens with a multi-channel SPR sensor. Biosens Bioelectron. 2006;22(5):752–8. https://doi.org/10.1016/j.bios.2006.03.012.
76. Teixeira LSG, Leão ES, Dantas AF, Pinheiro HLC, Costa ACS, De Andrade JB. Determination of formaldehyde in Brazilian alcohol fuels by flow-injection solid phase spectrophotometry. Talanta. 2004;64(3):711–5. https://doi.org/10.1016/j.talanta.2004.03.047.
77. Ung T, Liz-Marzán LM, Mulvaney P. Optical properties of thin films of Au/SiO_2 particles. J Phys Chem B. 2001;105(17):3441–52. https://doi.org/10.1021/jp003500n.
78. Wang Q, Wang JF, Geil PH, Padua GW. Zein adsorption to hydrophilic and hydrophopic surfaces investigates by surface plasmon resonance. Biomacromolecules. 2004;5(4):1356–61. https://doi.org/10.1021/bm049965r.
79. Wang X, Si Y, Wang J, Ding B, Yu J, Al-Deyab SS. A facile and highly sensitive colorimetric sensor for the detection of formaldehyde based on electro-spinning/netting nano-fiber/nets. Sensors Actuators B Chem. 2012;163(1):186–93. https://doi.org/10.1016/j.snb.2012.01.033.
80. Wang Y, Ou JZ, Chrimes AF, Carey BJ, Daeneke T, Alsaif MMYA, et al. Plasmon resonances of highly doped two-dimensional MoS_2. Nano Lett. 2015;15(2):883–90. https://doi.org/10.1021/nl503563g.
81. Wang J, Zhang HZ, Li RS, Huang CZ. Localized surface plasmon resonance of gold nanorods and assemblies in the view of biomedical analysis. TrAC. 2016a;80:429–43. https://doi.org/10.1016/j.trac.2016.03.015.
82. Wang X, Sun G, Li N, Chen P. Quantum dots derived from two-dimensional materials and their applications for catalysis and energy. Chem Soc Rev. 2016b;45(8):2239–62. https://doi.org/10.1039/c5cs00811e.
83. Wang W, Ramezani M, Väkeväinen AI, Törmä P, Rivas JG, Odom TW. The rich photonic world of plasmonic NP arrays. Mater Today. 2018;21(3):303–14. https://doi.org/10.1016/j.mattod.2017.09.002.
84. Wang Y, Jin Y, Zhang T, Huang Z, Yang H, Wang J, Jiang K, Fan S, Li Q. Emission enhancement from CdSe/ZnS quantum dots induced by strong localized surface plasmonic resonances without damping. J Phys Chem Lett. 2019a;10(9):2113–20. https://doi.org/10.1021/acs.jpclett.9b00818.

85. Wang H, Rao H, Luo M, Xue X, Xue Z, Lu X. Noble metal NPs growth-based colorimetric strategies: from monocolorimetric to multicolorimetric sensors. Coord Chem Rev. 2019b;398:113003. https://doi.org/10.1016/j.ccr.2019.06.020.
86. Watts HJ, Partes H, Yeung D. Real-time detection and quantification of DNA hybridization by an optical biosensor. Anal Chem. 1995;67(23):4283–9. https://doi.org/10.1021/ac00119a013.
87. Wätzig H, Oltmann-Norden I, Steinicke F, Alhazmi HA, Nachbar M, El-Hady DA, et al. Data quality in drug discovery: the role of analytical performance in ligand binding assays. J Comput Aided Mol Des. 2015;29(9):847–65. https://doi.org/10.1007/s10822-015-9851-6.
88. Wetchakun K, Samerjai T, Tamaekong N, Liewhiran C, Siriwong C, Kruefu V, Wisitsoraat A, Tuantranont A, Phanichphant S. Semiconducting metal oxides as sensors for environmentally hazardous gases. Sensors Actuators B Chem. 2011;160(1):580–91. https://doi.org/10.1016/j.snb.2011.08.032.
89. Wiley BJ, Im SH, Li ZY, McLellan J, Siekkinen A, Xia Y. Maneuvering the surface plasmon resonance of silver nanostructures through shape-controlled synthesis. J Phys Chem B. 2006;110(32):15666–75. https://doi.org/10.1021/jp0608628.
90. Wu F, Thomas PA, Kravets VG, Arola HO, Soikkeli M, Iljin K, et al. Layered material platform for surface plasmon resonance biosensing. Sci Rep. 2019;9(1):20286. https://doi.org/10.1038/s41598-019-56105-7.
91. Wu MC, Kao CK, Lin TF, Chan SH, Chen SH, Lin CH, et al. Surface plasmon resonance amplified efficient polarization-selective volatile organic compounds CdSe-CdS/Ag/PMMA sensing material. Sensors Actuators B Chem. 2020;309:127760. https://doi.org/10.1016/j.snb.2020.127760.
92. Xue S, Jiang XF, Zhang G, Wang H, Li Z, Hu X, et al. Surface plasmon-enhanced optical formaldehyde sensor based on CdSe@ZnS quantum dots. ACS Sensors. 2020;5(4):1002–9. https://doi.org/10.1021/acssensors.9b02462.
93. Yang Y, Miller OD, Christensen T, Joannopoulos JD, Soljačić M. Low-loss plasmonic dielectric nanoresonators. Nano Lett. 2017;17(5):3238–45. https://doi.org/10.1021/acs.nanolett.7b00852.
94. Yang W, Liu Y, McBride JR, Lian T. Ultrafast and long-lived transient heating of surface adsorbates on plasmonic semiconductor nanocrystals. Nano Lett. 2021;21(1):453–61. https://doi.org/10.1021/acs.nanolett.0c03911.
95. Yu H, Peng Y, Yang Y, Li ZY. Plasmon-enhanced light–matter interactions and applications. Npj Comput Mater. 2019;5(1):1–14. https://doi.org/10.1038/s41524-019-0184-1.
96. Zdanowicz M, Mroczyński R, Szczepański P. Strong second-harmonic response from semiconductor–dielectric interfaces. Appl Opt. 2021;60(5):1132. https://doi.org/10.1364/ao.414255.
97. Zemel JN, Jensen JD, Schoolar RB. Electrical and optical properties of epitaxial films of PbS, PbSe, PbTe, and SnTe. Phys Rev. 1965;140(1A):A330. https://doi.org/10.1103/PhysRev.140.A330.
98. Zhang H, Cao P, Dou J, Cheng L, Niu T, Zhang G. Double-exponential RI sensitivity of metal-semiconductor core-shell NPs: the effects of dual-plasmon resonances and red-shift. RSC Adv. 2018;8(3):1700–5. https://doi.org/10.1039/c7ra11981j.